Preferentially Oriented Submicron Silicalite Membranes

Mark C. Lovallo and Michael Tsapatsis
Dept. of Chemical Engineering, University of Massachusetts, Amherst, MA 01003

An oriented submicron silicalite membrane has been prepared by growing a layer of oriented silicalite crystals on a composite precursor nanocrystalline silicalite/alumina film using controlled secondary growth. The orientation of the crystals at the surface was such that both straight and sinusoidal channel networks run nearly parallel to the membrane surface. The membrane exhibits ideal selectivities for H_2 over N_2 as high as 60 at 150°C and O_2 over N_2 as high as 3.6 at 185°C. H_2, N_2 and O_2 permeances are 2.13, 0.05 and 0.17 $cm^3(STP)/(cm^2 \cdot min \cdot atm)$ at 185°C, respectively, and the corresponding apparent activation energies are 11, 26 and 32 kJ/mol. The permeation characteristics are attributed to the preferred orientation of the molecular sieving layer.

Introduction

Current commercial use of zeolites includes catalysis, ion exchange, and adsorption/separations (Davis, 1991). In all these applications, the zeolite is utilized in its powder form. In particular, gas separation by zeolites is performed by pressure swing adsorption (PSA) where separation relies on the preferential adsorption of one component (usually the desired component) over another. Replacing this unsteady process with a continuous process has been one driving force for the development of zeolite membranes. Their potential uses as membrane reactors (combined reaction-separations), selective sensors (Yan and Bein, 1995, 1992a,b; Bein and Brown, 1989), and optoelectronic materials (Ozin et al., 1989; Caro et al., 1992) has provided additional interest for the formation of molecular sieve films.

For molecular sieving applications, the ideal configuration of a zeolite membrane would be a thin (< 1 μm), dense (no interzeolitic porosity), and appropriately oriented zeolite layer. Other obstacles, besides the synthesis of suitable zeolite membranes, to be overcome for the commercialization of such materials are discussed in a recent review by Zones and Davis (1996).

The two most prevalent techniques that have been implemented for the fabrication of zeolite containing membranes are post-preparative (*ex-situ*) and *in-situ* methods. Post-preparative methods involve the incorporation of a powdered zeolite into a glassy polymer or inorganic matrix (Bein et al., 1989). The pioneering work of Hennepe et al. (1987) showed how the addition of the hydrophobic zeolite silicalite to a silicone rubber (PDMS) membrane increased the selectivity of alcohols over water during pervaporation. In a later report, Hennepe et al. (1994) experimentally determined the concentration profiles of permeants across the PDMS/silicalite membrane. It was concluded that for these heterogeneous membranes, diffusion through the membrane determines the rate of transport, that is, adsorption/desorption is a fast process.

Following this work, Jia et al. (1991) constructed a similar membrane that displayed enhanced O_2/N_2 selectivity. The addition of silicalite to a PDMS matrix facilitated the transport of smaller molecules through the membrane. The O_2/N_2 ideal selectivity was found to increase from 2.15 to 2.92 with increasing zeolite (silicalite) content up to 70 wt. %.

Other researchers have investigated the sorption and diffusion of permeates like acetic acid (Netke et al., 1995) and chlorinated hydrocarbons (Dotremont et al., 1995) in these composite (silicalite/PDMS) membranes, as well as the use of polyimide (Vankelecom et al., 1995) as a matrix instead of PDMS. One recent publication reported the catalytic esterification of acetic acid carried out in a composite zeolite A/polyvinyl alcohol (PVA) membrane (Gao et al., 1996).

The strength and flexibility of these composite zeolite/polymer membranes eases their implementation in permeation and membrane reactor apparatuses. However, membrane performance (that is, selectivity, permeance) as well as the thermal and chemical stability limitations imposed by the

Correspondence concerning this article should be addressed to M. Tsapatsis.

polymer matrix drive the search for pure zeolitic films or inorganic/zeolite composite films.

Preparation of pure zeolitic and/or inorganic/zeolite composite membranes has mostly been investigated using *in-situ* techniques. This method consists of placing a suitable substrate in contact with a precursor solution or gel. A zeolite film is then grown on the substrate through hydrothermal treatment. Using this technique, layers of ZSM-5 (Anderson et al., 1992; Sano et al., 1992; Masuda et al., 1994), silicalite (Meriaudeau et al., 1995; Noble and Falconer, 1995), zeolite A (Masuda et al., 1995; Yamazaki and Tsutsumi, 1995; Kita et al., 1995), zeolite Y (Valtchev et al., 1995), and ferrierite (Matsukata et al., 1994) have been grown on various supports. In some cases zeolite films have been formed on the Teflon lining of the reaction vessel and were removed and used as self-supported films (Tsikoyiannis and Haag, 1992). A recent report by Jansen and Coker (1996) reviews some of these studies regarding zeolite membrane preparation and characterization.

For separation applications, zeolite film growth has been achieved on porous substrates such as porous alumina, stainless steel, and clay supports. The majority of work in this area has focused on composite silicalite or ZSM-5 membranes. Geus et al. (1992, 1993) were able to grow continuous layers of silicalite (50–100-μm-thick) on both porous clay and stainless steel. The film was composed of multilayers of randomly oriented intergrown silicalite crystals with grain sizes of approximately 20 μm. Permeation experiments revealed a sequence for single gas permeabilities at room temperature as methane $>$ *n*-butane $>$ neon $\gg$ isobutane. Using binary mixtures, the membrane was found to be selective for *n*-butane (strongly adsorbed) over methane (weakly adsorbed) demonstrating that permeation is based on both adsorption and diffusion. While these membranes exhibited molecular-sieving effects, Geus et al. did not exclude the possible existence of larger (intercrystalline) pores.

Sano et al. (1991, 1994) have extensively reported on the preparation and characterization of ZSM-5 and silicalite films on porous stainless steel, alumina, and Teflon. The supported membranes ($\sim$ 500-μm-thick) were composed of randomly oriented, intergrown crystals. The authors also indicated the presence of intercrystalline porosity. The potential use of these membranes for separation of water/alcohol and methanol/MTBE mixtures by pervaporation was examined (Sano et al., 1995). In both cases, the membrane showed selectivity for the more strongly adsorbed alcohol.

Also using *in-situ* growth, a continuous silicalite membrane was prepared on the inside of a porous alumina tube by Bai et al. (1995). The 10-μm-thick layer exhibited molecular sieving properties and activated diffusion for several pure gases (apparent activation energies in the range of 8.5–16.2 kJ/mol). In a more recent study Funke et al. (1996) investigated the separation of higher boiling point organic compounds with a similar zeolite membrane. The investigators found a separation selectivity of 40 for *n*-octane over isooctane at $\sim$ 413 K for a mixture of the two components diluted with *n*-hexane. In the absence of *n*-hexane the selectivity of *n*-octane over isooctane was only 8. Also, in single gas measurements isooctane permeated up to 5 times faster than *n*-octane. The authors attribute the mixed feed permeation characteristics to nonideal adsorption behavior. The same research group (Baertsch et al., 1996) has recently reported on dramatic changes in selectivity through these membranes when measurements were performed with single vapors and mixtures. That behavior was attributed to single-file diffusion.

The preparation of a ZSM-5 membrane supported on porous alumina discs has been presented by Yan et al. (1995a,b). The porous alumina disc was elevated in the synthesis mixture, face down, to prevent deposition of crystalline particles on the substrate through settling in the solution. The *in-situ* grown membranes consisted of a 10-μm-thick polycrystalline film. The film is thought to nucleate in the pore mouth of the substrate, penetrating at a depth of several microns below the surface. Permeation of a variety of pure gases was measured with ideal selectivities as high as 151 for hydrogen/*i*-butane and 31 for *n*-butane/*i*-butane.

Kapteijn et al. (1995) reported on the preparation and characterization of a silicalite membrane grown over a stainless steel gauze. From single gas permeation measurements, the ideal selectivity of hydrogen over *n*-butane was 20. Binary experiments, however, showed a selectivity toward *n*-butane at 300 K with fluxes of 0.2 and 1.0 mmol/m^2/s for hydrogen and *n*-butane, respectively. At higher temperatures (600 K), the membrane selectivity favors hydrogen with fluxes of 25 and 10 mmol/m^2/s for hydrogen and *n*-butane, respectively.

These reports of *in-situ* grown supported membranes show promising advances in film quality and permeation characteristics. The control of film microstructure, however, is somewhat limited with zeolite films most commonly comprised of several layers of randomly oriented crystals. In addition, film thicknesses of less than one micron need to be achieved to overcome low flux limitations and fully realize the potential of these devices.

The growth of more oriented zeolite layers has been achieved by Jansen and Rosmalen (1993), Feng and Bein (1994), and more recently by Yan et al. (1996). The report by Jansen and Rosmalen shows a continuous film, buildup of *in-situ* grown silicalite crystals ($\sim$ 2 μm in length), on silicon wafers. The crystals are aligned with their (010) faces parallel to the substrate. The crystals do not appear to be highly intergrown and interzeolitic porosity exists. By altering synthesis conditions, Jansen et al. (1994) have been able to obtain a very thin (300 nm) and intergrown (no intercrystal porosity visible by SEM) layer of silicalite on silicon. The crystal grains in this case do not have well-developed facets but do display some extent of orientation. The formation of a similar film on a porous substrate has not yet been reported.

All of the above reports have addressed certain aspects desirable for the preparation of an "ideal" molecular sieving zeolite membrane. However, combining some of the more important film characteristics, that is, density (no interzeolitic porosity), thickness ($<$ 1 μm), and preferred orientation, remains an elusive goal.

We proposed the use of zeolite colloidal suspensions (Tsapatsis et al., 1995a) as precursors to zeolite membrane formation. The processing scheme we developed involves the preparation of nanocrystalline zeolites and zeolite nanosols (colloidal suspensions of nanocrystalline zeolites). The nanosols are used for film deposition resulting in either unsupported or supported zeolite films. These films are composed of packed zeolite particles with interzeolitic pores on the order of the particle size. To close the interzeolitic poros-

ity at the surface, a seeded growth procedure (which we refer to as secondary growth) is implemented. Starting from nanocrystalline zeolite L suspensions, we have previously reported on the preparation of an asymmetric zeolite L film (Tsapatsis et al., 1995b, 1996; Lovallo and Tsapatsis, 1996; Lovallo et al., 1996a,b). The film described has decreasing crystal grain size and increasing interzeolitic porosity from the surface to the interior of the film. The surface is composed of a thin (~ 200 nm) layer of highly intergrown, randomly oriented zeolite L crystals.

In what follows, we describe a similar procedure for the preparation of a thin, oriented, molecular sieving silicalite membrane. Insight into synthesis procedures and membrane characterization are presented. Pure gas permeation and temperature dependence characteristics were obtained and analyzed.

Experimental Studies

Silicalite nanosol preparation

Silicalite particles of approximately 100 nm in size were hydrothermally prepared using tetrapropylammonium hydroxide (TPAOH, 1.0 M Aldrich), fumed silica (Cab-O-Sil Grade 5-M), and sodium hydroxide (NaOH, Aldrich). Approximately 0.85 g of NaOH was added to 60 mL of 1.0-M TPAOH and stirred at room temperature in a flask until dissolved. 15 grams of fumed silica was then added to the solution to form a slurry. The slurry was heated at 80°C until clear while approximately 10 g of water was evaporated off the solution. The resulting mixture was clear with a composition of 10 SiO_2 : 2.4 TPAOH : 1 NaOH : 110 H_2O. The solution was placed in Teflon-lined stainless steel autoclaves and rotated in an oven at 125°C for 8 h. After cooling, a stable aqueous suspension was prepared by repeated washing with DI water and centrifuging until the pH of the sol was neutral with a zeolite concentration of 20 (g silicalite)/L.

Precursor film casting

Composite silicalite/alumina unsupported films were prepared by mixing calculated amounts of aqueous silicalite (20 g/L) and boehmite suspensions (30 g/L). The two suspensions were mixed in a flask at room temperature under stirring. The mixed dispersion was then poured into a casting dish [flat bottomed petri-dish, 2 in. (51 mm) in diameter, 1 in. (25 mm) high] and left open to atmosphere at room temperature. Films of different thickness were obtained by adding more of the mixed dispersion to the casting dish before all the solvent had evaporated. Recovered films were ~ 2 cm in diameter and ~ 1–2 mm thick. The films were dried at 110°C and then calcined at 750°C for 4 h.

Supported films were obtained by dip coating precleaned glass slides (VWR) and silicon wafers with the mixed silicalite/boehmite dispersion. The substrates were immersed into the dispersion for approximately 2 min. The slide was then removed at a rate of 1 cm/min and subsequently dried at 40°C. The dip procedure was repeated up to 5 times. After the final dipping, the coated slide was dried at 110°C and then slowly heated to 550°C and held for 6 h. Both unsupported and supported precursor films are polycrystalline and randomly oriented.

Secondary growth

For silicalite particle secondary growth, calculated amounts of silicalite sol (20 g/L), tertraethyl orthosilicate (TEOS, Aldrich), TPAOH, and DI water were mixed under stirring at room temperature in a flask with a resulting composition of 40 SiO_2 : 12 TPAOH : 16800 H_2O : 40 g silicalite. The mixture was placed in Teflon-lined stainless steel autoclaves and heated in a rotating oven at 130°C for 8 h. After cooling, solid products were recovered by repeated washing and centrifuging followed by drying at 110°C overnight.

For membrane preparation, the same procedure was followed except calcined pieces of unsupported silicalite/alumina (90 wt. %/10 wt. %) film or supported film were used in place of silicalite particles. Films were removed from the oven at various times and left in a DI water bath overnight. After this washing, the unsupported films were dried at 110°C and calcined at 750°C for 2 h.

Characterization

XRD patterns of both solid products and supported films were collected on a Scintag XDS-2000 diffractometer in Bragg Brentano geometry equipped with a liquid nitrogen cooled germanium detector using Cu Kα radiation. Supported films were analyzed with the film surface perpendicular to the plane of the X-ray source and detector.

TEM micrographs were taken on a JEOL 100CX microscope operating in TEM mode at 100 kV. Specimens for TEM were prepared by dispersing the sample in ethanol and depositing a drop of the suspension on a carbon coated grid.

SEM photographs were recorded on a JEOL 100CX microscope operating in SEM mode at 20 kV. Samples were prepared by attaching film and membrane pieces to the specimen holder with conductive carbon tape followed by sputtering a gold coating.

Single gas permeation

Permeances were measured for precursor silicalite/alumina films and secondary grown silicalite/alumina membranes (calcined and uncalcined). One side of the films was slightly polished to remove any film created during secondary growth on that side. The membranes were then attached to a glass plate (3 cm × 3 cm) with Varian Torr Seal epoxy. The glass plate was then attached to a glass tube with the same epoxy. A hole in the glass plate (5 mm in diameter) allowed for flow of gases from the feed side, through the membrane, to the permeate side. Figure 1 illustrates the connection of the membrane to the glass plate and the permeation apparatus. The membrane housing was placed in a temperature controlled tube furnace. Initially, the permeate side is at vacuum and the feed side is at 1 atm with a feed gas flow rate of approximately 10 cm^3/min. The permeate side is then isolated from vacuum and the rate of change in pressure was measured with a pressure transducer. The permeance (P) of the membrane was calculated from the volume flow rate (Q), the membrane area (A), and the pressure difference (Δp) across the membrane

$$P = Q/(A\Delta p) \qquad (cm^3/cm^2\text{-min-atm}) \qquad (1)$$

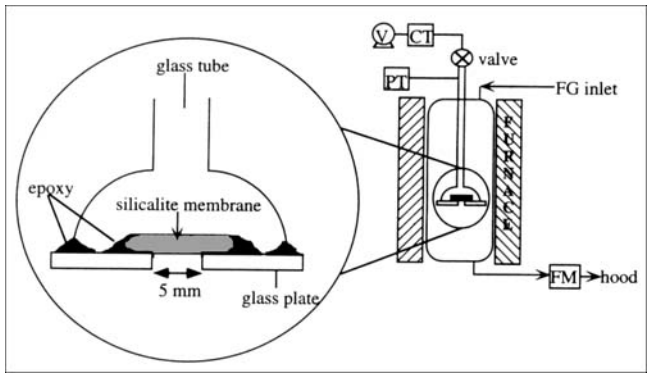

Figure 1. Permeation apparatus.

V-vacuum pump; CT-cold trap; PT-pressure transducer; FG-feed gas; FM-flowmeter.

The flow rate is calculated from the recorded change in pressure with time

$$Q = \frac{(\Delta p/\Delta t) \times DV \times 22{,}414}{RT} \quad (\text{cm}^3/\text{min}) \qquad (2)$$

where Q is the volume flow rate (cm^3/min), $\Delta p/\Delta t$ is the recorded rate of pressure change (atm/min), DV is the volume in the permeate side of the apparatus (cm^3), R is 82.0578 (cm^3·atm/mol·K), and T is the temperature (K).

All measurements were taken in the range of 0–3 torr at permeate side and 1 atm at feed side. Several runs were made for each gas at each temperature followed by H_2 after every gas to check for consistency. Depending on the gas, different equilibration times (up to 12 h) were required when switching from one gas to another to reach a constant permeance value.

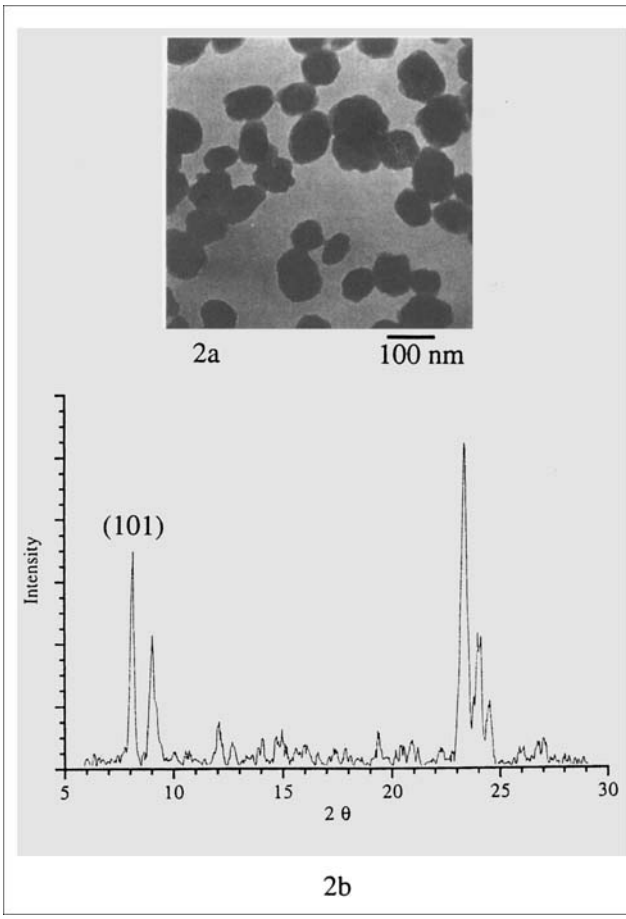

Figure 2. Silicalite nanocrystals.

(a) TEM micrograph (100,000×); (b) powder XRD pattern.

Results and Discussion

Silicalite synthesis

The nanocrystalline silicalite is formed from a clear homogeneous solution. The resulting product is a milky suspension of the silicalite in its mother liquor. By washing to a pH of 7, a stable silicalite sol is prepared. Figures 2a and 2b show a TEM image and a powder XRD pattern of the dried silicalite particles. From XRD line broadening calculations performed on the (101) peak using the Scherrer equation, the average grain size of the particles is found to be approximately 30 nm. The TEM image reveals particle sizes of around 100 nm. The smaller size as determined by XRD suggests that the particles consisted of smaller single crystalline domains.

Precursor silicalite film

Figure 3 shows an SEM top view of an unsupported piece of composite silicalite (90 wt. %/alumina (10 wt. %) film. The size of the particles is consistent with TEM observations ($\sim$100 nm). The film is composed of well-packed silicalite particles, leaving interzeolite spacings on the order of the particle size. The alumina is in small quantity and too finely divided to be seen in the SEM image. This particular film is approximately 2 cm in diameter, 2 mm thick, and white in color. The film thickness can be controlled by the concentration and quantity of zeolite suspension poured into the casting dish. Thinner films are more translucent but generally too fragile to perform permeation measurements, and thicker films require longer casting times and more silicalite suspension. Prior to calcination, even 2-mm-thick films are fairly delicate and will fall apart if exposed to water. After calcining, the film samples exhibit increased mechanical and chemical strength with no change in color or size and shape. The enhanced strength which allows for easy manipulation of the films is attributed to the small amount of alumina that presumably forms strong chemical bonds between individual silicalite particles upon calcination. The exact nature and phase of the alumina is unknown at this time because it is undetectable in the XRD patterns and TEM micrographs. XRD analysis of calcined silicalite particles indicate no change upon calcination except for the removal of the occluded organic (TPA) at this temperature.

Secondary growth

For molecular sieving applications, the interzeolitic porosity of these silicalite membranes needs to be closed, leaving transport pathways only through the silicalite crystals. Using the same principle as demonstrated for the processing of zeolite L films (Lovallo et al., 1996b), synthesis conditions were identified where the silicalite particles grow larger in a seeded

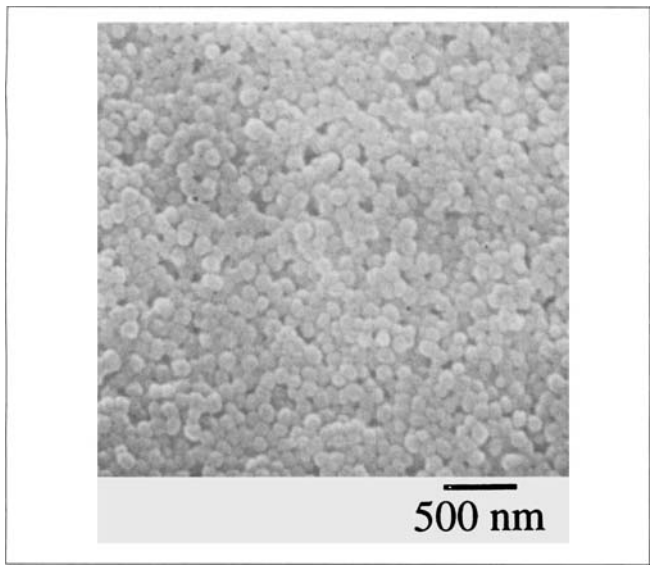

Figure 3. Precursor silicalite/alumina film.
SEM top view (20,000×).

hydrothermal treatment (we call this process secondary growth). Figures 4a and 4b show a TEM micrograph of the silicalite particles after secondary growth along with the corresponding XRD pattern. By comparing to Figure 2, it is evident the particles have grown larger to approximately 150–200 nm in size after 8 h of secondary growth. Under these regrowth conditions, the particles grow as plates with the longest edge being along the crystallographic c-axis.

The next step was to expose the calcined pieces of composite silicalite/alumina film to the same secondary growth conditions. The goal is to cause the silicalite particles in the film to grow larger, closing the interzeolitic spacing, and forming a molecular sieving membrane. Figure 5 shows a series of SEM top views and cross-sections taken at various times throughout the secondary growth process. After 4 h of heating (Figure 5a), some larger crystal grains appear dispersed across the film surface. Upon further heating, the crystals at the surface grow larger and cover more of the surface. At 6 h, the surface is not yet completely covered with the crystal grain size being around 500 nm as observed in the SEM micrograph of Figure 5b. Also evident at this time is a preferred orientation of the majority of crystals with their straight channel direction (crystallographic b-axis) parallel to the film surface. After 9 h of heating (Figures 5c and 5d), a continuous and intergrown layer has formed at the film surface. From the SEM top view of Figure 5c, the crystal grain size at the surface appears to be 750 nm. The orientation of the surface crystals is even more evident in this figure with the crystallographic b-axis parallel to the film surface. Figure 5d shows an SEM cross-section of the same sample after 9 h of secondary growth. This view reveals a thin intergrown layer supported on the original precursor composite film. Below the intergrown layer, the silicalite crystals appear to have experienced little or no regrowth. This figure also indicates that the top layer is one crystal thick. That is, the silicalite grain size in the intergrown layer is of the same magnitude as the top layer thickness (~ 750 nm). At 24 h of secondary growth, the crystal grain size and corresponding surface layer thickness have increased to 2 μm, as shown in Figures 5e and 5f. Because the film thickness is approximately equal to the crystal grain size at the surface, film growth does not seem to proceed by the multilayer deposition of crystalline particles from the solution phase to the film surface. A similar microstructure was observed in zeolite L films using a similar procedure (Lovallo et al., 1996b). However, because under the regrowth conditions used here silicalite crystals can form in the solution phase, it is unknown whether the layer formation proceeds by the secondary growth of silicalite particles in the precursor film or by the deposition of a single layer of small silicalite crystals from the solution phase which continue to grow into a continuous layer. A combination of both these mechanisms may also be possible.

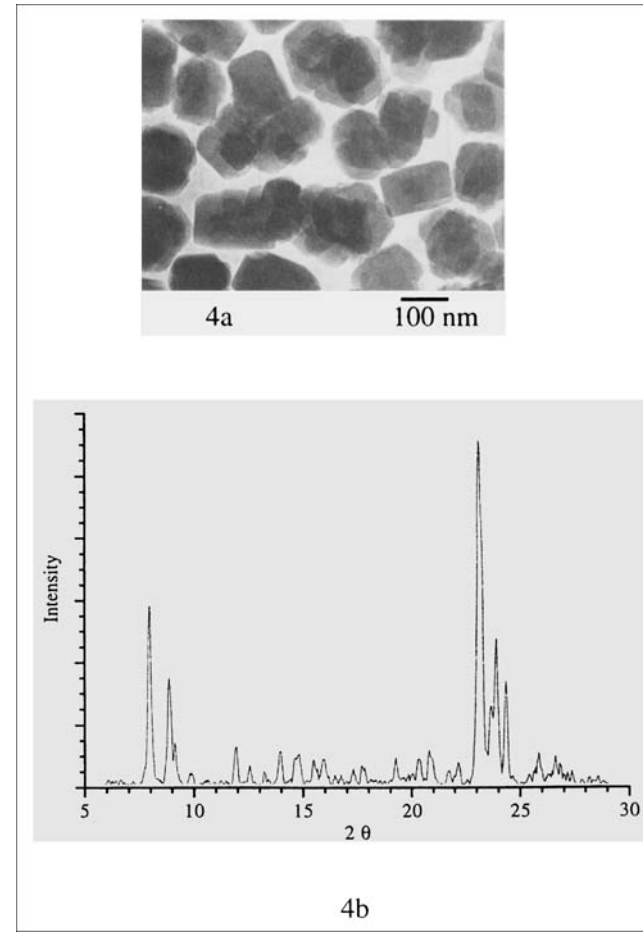

Figure 4. Regrown silicalite nanocrystals.
(a) TEM micrograph (100,000×); (b) powder XRD pattern.

To demonstrate the role of the precursor composite film, a series of experiments were performed under the same conditions used in the secondary growth process. In this case, other substrates (glass, silicon, alumina plate, and zirconia) were used in place of the precursor silicalite film. In all instances, crystals with similar morphologies as those seen in Figure 5 were found on the surface of the substrates. However, the crystals were always found in a very low coverage and never formed an intergrown layer even after long heating times (48 h). Figure 6 shows an SEM top view of a bare silicon wafer

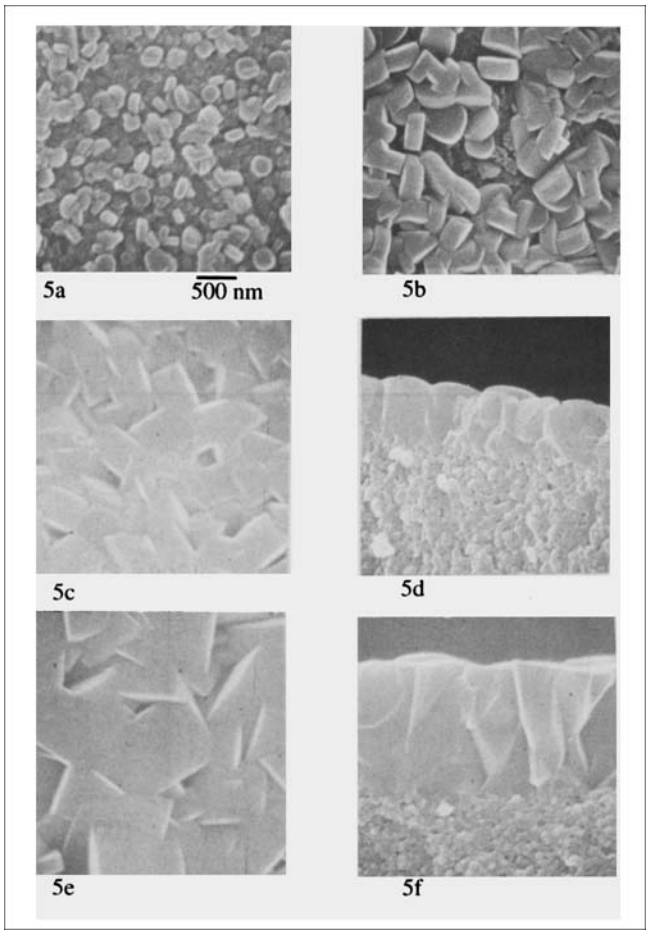

Figure 5. Secondary growth of precursor silicalite/alumina film.

(a) SEM top view after 4 h of heating; (b) SEM top view after 6 h of heating; (c) SEM top view after 9 h of heating; (d) SEM cross section after 9 h of heating; (e) SEM top view after 24 h of heating; (f) SEM cross section after 24 h of heating.

that was subjected to the same secondary growth conditions for 24 h as used on the precursor silicalite/alumina films. The crystals are found with two orientations, the crystallographic b-axis parallel or perpendicular to the substrate surface, but they do not form a continuous layer. Figure 7 shows SEM top views and cross-sections of a silicon and a glass substrate that were first dip-coated with a layer of silicalite/alumina and then exposed to secondary growth. The supported film on Si was exposed to secondary growth conditions for 8 h (Figures 7a and 7b), while the supported film on glass was heated for 24 h (Figures 7c and 7d). In both cases, the precoated substrates result in films with similar morphologies as those seen in Figure 5 suggesting no particular influence of the substrate. This indicates that, while crystals may deposit from the solution phase during secondary growth, the precursor silicalite film or layer surface plays some crucial role in the development of the oriented intergrown layer, either by the secondary growth of silicalite crystals in the precursor film or by providing a surface which favors deposition and attachment of crystals from the solution.

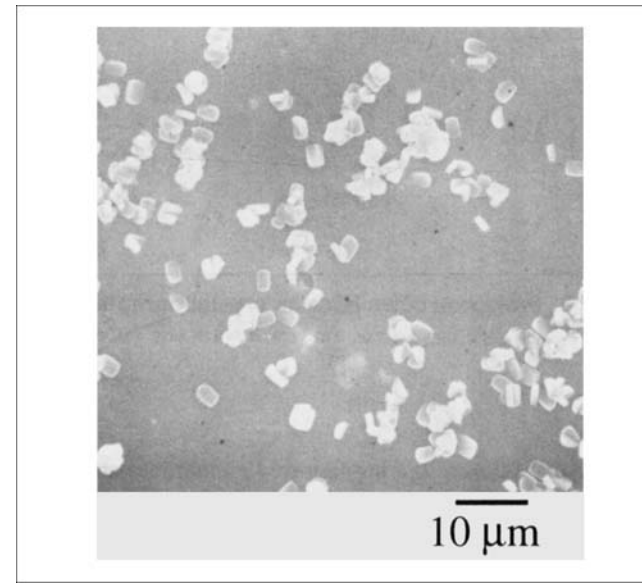

Figure 6. Silicon wafer heated in secondary growth conditions.

Crystal orientation

From the SEM pictures of Figure 5, it is evident that the intergrown surface crystals formed during secondary growth have a preferred orientation. To examine the orientation in more detail, analysis by XRD was performed on similar sili-

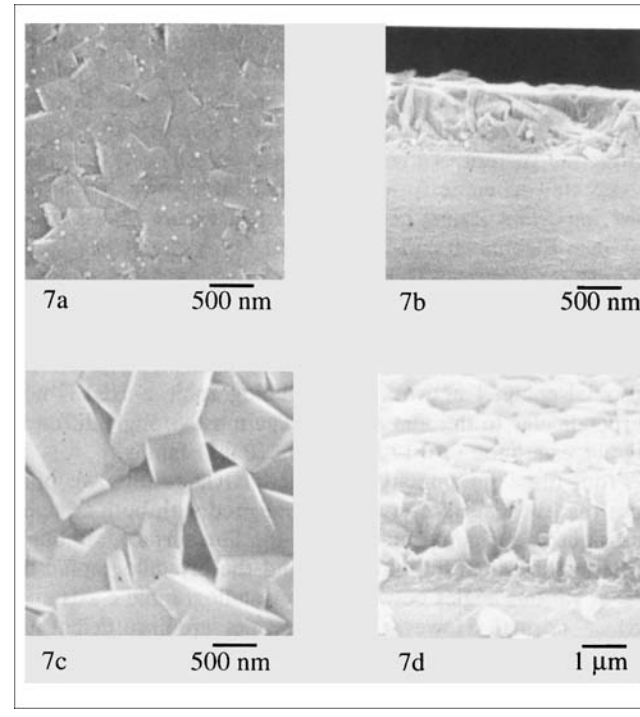

Figure 7. Precoated substrates subjected to secondary growth.

(a) SEM top view of precoated Si wafer heated for 8 h; (b) SEM cross section of precoated Si wafer heated for 8 h; (c) SEM top view of precoated glass slide heated for 24 h; (d) SEM cross section of precoated glass slide heated for 24 h.

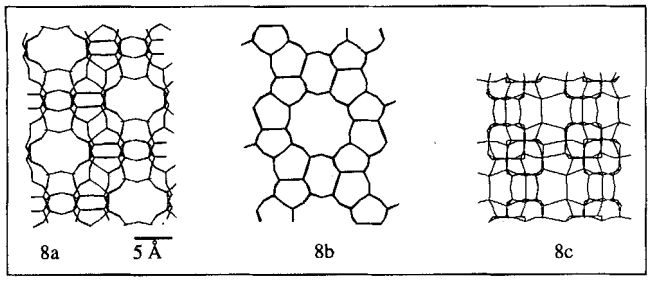

Figure 8. Projection down silicalite crystallographic axes.

(a) View down a-axis; (b) view down b-axis; (c) view down c-axis.

calite layers. Because the unsupported membranes are only a few cm in diameter and are not perfectly flat, the supported silicalite layer on glass, as shown in Figures 7c and 7d, was used to provide a large flat surface for XRD examination. For reference, Figures 8a, 8b, and 8c show a stick model of silicalite viewed down the sinusoidal channels (crystallographic a-axis), the straight channels (crystallographic b-axis), and the crystallographic c-axis, respectively. Direct transport pathways are evident in the crystallographic a and b-direction. No channels transverse the crystallographic c-axis, although transport in this direction is possible by jumping between the straight and sinusoidal channel networks.

Figure 9 shows an XRD pattern taken from a precoated glass substrate prior to secondary growth (Figure 9a), and from the silicalite layer shown in Figure 7c (Figure 9b). For these measurements, the sample was placed in the sample holder with the film surface perpendicular to the plane of the X-ray source and detector. With this geometry, only planes that are parallel or nearly parallel to the film surface will be seen in the corresponding XRD pattern. The underlying nanocrystalline particles are expected to contribute to the diffraction pattern of Figure 9b, however, most of the signal is expected to come from the thicker intergrown top layer. One important aspect of the pattern in Figure 9b, as compared to Figures 2b and 9a, is that the majority of peaks are from (h 0 1) planes. This suggests that the straight channel network of the crystals (or crystallographic b-axis) is parallel to the film surface. There is also no evidence of intense reflections from any (h 0 0) planes which indicates that the sinusoidal channel network (or crystallographic a-axis) is not perpendicular to the film surface. The most strongly diffracting planes are the ⟨1 0 1⟩ family and ⟨0 0 1⟩ family.

From these preliminary SEM and XRD results, we propose that most surface crystals are aligned with both straight and sinusoidal channels parallel to the film surface, although some may be slightly "tilted" around the crystallographic b-axis at various angles between the crystallographic c-axis and surface normal. However, these results are insufficient to provide a quantitative analysis of the orientation distribution of the film top layer. We are currently using thin film and pole figure XRD analyses to more accurately describe the orientation of these zeolite films. These results will be reported elsewhere. Moreover, although we refer to the top layer as silicalite, we cannot exclude possible contamination with aluminum leached in small amounts from the binder of the precursor film.

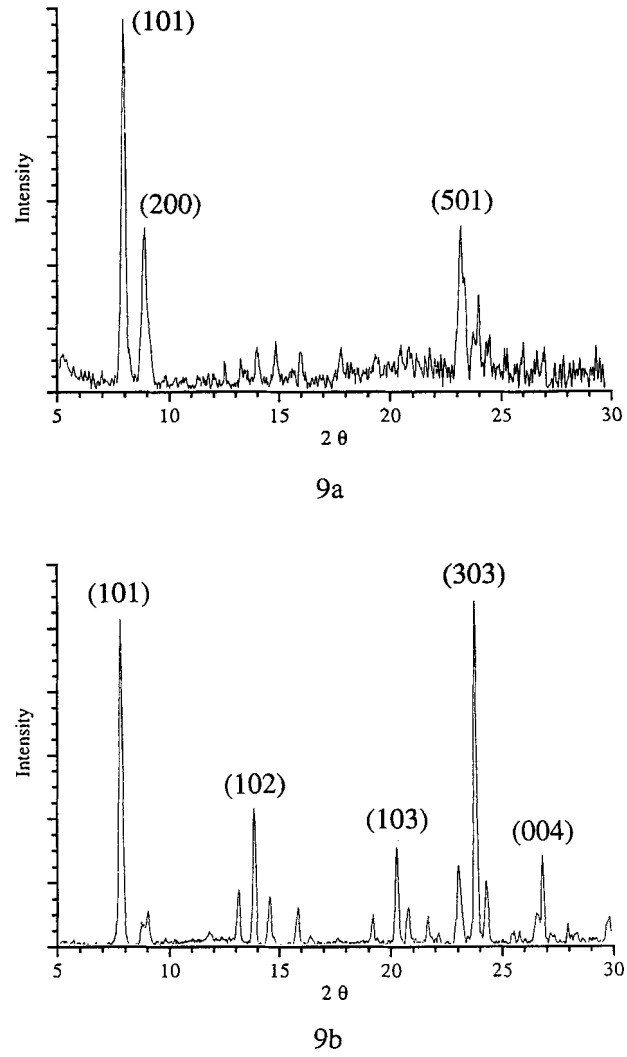

Figure 9. XRD analysis of crystal orientation.

(a) XRD pattern taken of precoated glass prior to secondary growth; (b) XRD pattern taken of silicalite film formed on precoated glass after 24 h of secondary growth.

Single gas permeation

Table 1 shows the permeances of a precursor composite silicalite/alumina membrane (prior to secondary growth) and of the composite silicalite/alumina membrane after secondary growth shown in Figures 5c and 5d (9 h secondary growth). Permeance characteristics of several silicalite/ZSM-5 membranes reported by other researchers have been included in the table for comparison. The precursor membrane shows selectivity for H_2 over N_2 of around 3, close to the selectivity expected for Knudsen diffusion being the main transport mechanism. The permeance decreases with increasing temperature for both gases, which is also indicative of Knudsen diffusion. This is consistent with SEM observations of the pore size in the precursor membrane (Figure 3) being < 100 nm.

The membrane after secondary growth and calcination exhibits N_2 permeances two orders of magnitude lower than that of the precursor film. Most notably, the permeance of H_2 is up to 60 times higher than that of N_2. Also, the perme-

Table 1. Single Gas Permeances: Silicalite/ZSM-5 Membranes

	Permeance × 10^2 cm^3 (STP)/(cm^2·min·atm)					
	H_2	N_2	O_2	*n*-Butane	*i*-Butane	
185°C	1,150	375	—	—		Precursor Silicalite/ Alumina Film This Work
150°C	167.0	2.7	8.4	4.7	2.4	
185°C	213.0	4.7	16.9	7.4	2.4	(9 h of sec. growth)
Ea (kJ/mol)	11	26	32			This work
185°C	137.6	54.5	55.7	79.4	2.6	(Yan et al., 1995)
20°C	316	103	—	13.6	2.2	(Jia et al., 1993)
145°C	213	47	54	—	—	(Geus et al., 1993)
25°C	5,980	2,120	—	104.7	34.0	(Jia et al., 1994)

ance of O_2 is 3.5 times higher than that of N_2 at 185°C. Selectivities for hydrogen and oxygen over nitrogen with silicalite/ZSM-5 membranes have been previously reported by other investigators, but at much lower values than presented here. The *n*-butane/*i*-butane selectivity for this membrane is only 2–4, which is lower than other work.

Based on the permeances in the temperature range 100–200°C, activation energies as high as 30 kJ/mol were calculated for N_2 and O_2 as reported in Table 1. Previous work has reported values in the range of 8–16 kJ/mol (Bai et al., 1995).

Tests performed with films that were not calcined showed almost no permeance (on the resolution of the apparatus) for any of the above gases. All of these results clearly indicate that molecular sieving is occurring through the thin (750 nm), intergrown, and oriented layer at the surface of the membrane. The unique permeation characteristics and effective activation energies are caused by the orientation of the silicalite crystals at the intergrown surface layer. Because the crystals are oriented with their straight and sinusoidal channels parallel to the membrane surface, transport through the membrane should occur by successive jumping between the two channel networks. In this respect, the silicalite layer performs as a small pore material rather than a medium pore zeolite.

Molecular dynamics (MD) calculations have indicated that for the diffusion of ethane in silicalite, there is a higher probability of the molecule continuing to move along a given channel direction than to randomly change from one channel system to another (Rees, 1994). MD calculations of methane and xenon in silicalite (June et al., 1990) predict the diffusivity in the direction of the straight channels to be an order of magnitude larger than in the direction perpendicular to both straight and sinusoidal channels. Measurements with methane in silicalite (Karger and Ruthven, 1992) show that the diffusivity in the crystallographic c-direction is smaller than the diffusivities in the straight and sinusoidal channels by a factor of 5 because the molecule must jump repeatedly between the two channel systems to diffuse. The smaller H_2 molecule may move much more readily between channels than the larger N_2 molecules accounting for the high selectivities reported here. The lower selectivities for N_2 and *n*-butane over *i*-butane compared to reported values for randomly oriented films suggest that, while N_2 and *n*-butane may move much more rapidly through a channel system than *i*-butane, the jumping between channels is nearly as likely for *i*-butane as compared to *n*-butane and N_2.

Table 2 lists some single gas permeance values for silicalite with thicker molecular sieving layers than that of the membrane reported in Table 1. The membranes with thicker layers showed similar selectivities but lower permeance at 185°C. However, the permeance is not inversely proportional to the layer thickness.

At this stage of development, regarding the reproducibility of the technique, we state that out of 5 membranes prepared under similar conditions, 4 showed molecular sieving properties and one membrane displayed Knudsen selectivity due to defects in the surface layer. Figure 10 shows an SEM picture of one of these defects. They are clearly not cracks propagated along the surface, but rather delamination of the top layer. They are most possibly caused by failure of the substrate layer at some stage of regrowth due to insufficient bonding. This type of crack is representative of the majority of defects found in all analyzed samples.

Inorganic amorphous silica membranes have previously been shown to be H_2 selective (Tsapatsis et al., 1991, 1992, 1994; Kim and Gavalas, 1995). Typical permeance values for these amorphous membranes are on the order of 0.1–2 cm^3 (STP)/(cm^2·min·atm) at 500°C. While permeances for the zeolite membranes described here were not measured above 200°C due to limitations imposed by the epoxy used in the permeation apparatus, extrapolation to higher temperatures suggests high permeation rates. However, the zeolite membrane selectivities are much lower than the dense amorphous membrane selectivities which can be as high as 1,000 for H_2 over N_2.

The overall size of these zeolite membranes is currently limited by the size of the precursor film (typically a few cm in diameter). For practical application, large membrane areas are needed and a way to overcome this limitation is to use

Table 2. Single Gas Permeance at 185°C for Silicalite Membranes of Various Thicknesses

Permeance × 10^2 cm^3 (STP)/(cm^2·min·atm)			
H_2	N_2	O_2	
167.0	2.7	4.7	~ 0.75-μm-thick layer
25.0	0.5	1.3	~ 1.5-μm-thick layer
25.0	0.5	1.5	~ 2-μm-thick layer

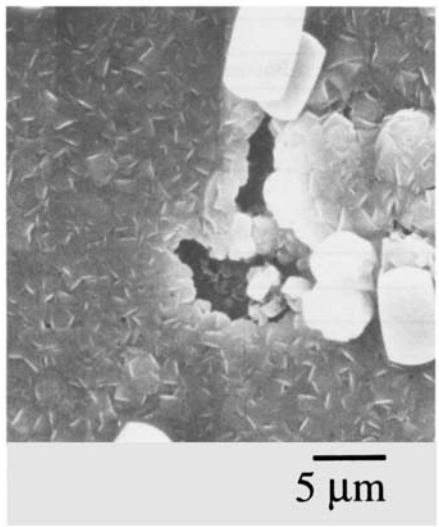

Figure 10. SEM picture of a defect found in a silicalite membrane.

commercial porous substrates like Vycor glass and asymmetric membranes like U.S. Filter membranes. We have reported that the preparation technique can be applied to such substrates (Lovallo et al., 1996a), and characterization of these composite membranes is underway.

To our knowledge, this is the first time that the preparation of submicron, oriented zeolite membranes with molecular sieving properties is demonstrated.

Conclusion

A composite silicalite membrane was formed by casting a precursor silicalite/alumina membrane from a silicalite nanosol followed by secondary growth. The resulting membrane has a thin (750 nm) intergrown and oriented molecular sieving layer at the surface. The surface crystals are oriented with their straight and sinusoidal channels parallel to the membrane surface. This microstructure produces the following permeation properties:

- Ideal selectivity for H_2 over N_2 as high as 60 and O_2 over N_2 as high as 3.5
- Activation energies for N_2 and O_2 as high as 30 kJ/mol.

These unique characteristics are attributed to the orientation of the surface layer forcing transport across the membrane to occur by jumping between straight and sinusoidal channel networks.

Secondary growth of precursor nanocrystalline zeolite layers with its successful demonstration in two distinct zeolite types (MFI, LTL) appears promising as a general method for preparation of molecular sieve films with controlled microstructure.

Acknowledgments

Acknowledgment is made to the donors of the Petroleum Research Fund, administered by the American Chemical Society and the NSF-ARI (CTS-9512485) Program for support of this research. Professor S. Suib and Mr. Niangao Duan are greatly appreciated for providing access to XRD facilities at the University of Connecticut. Finally, we acknowledge the W. M. Keck Polymer Morphology Laboratory for use of its Electron Microscopy Facilities.

Literature Cited

Anderson, M. W., K. S. Pachis, J. Shi, and S. W. Carr, "Synthesis of Self-supporting Zeolite Films," *J. Mater. Chem.*, **2**, 255 (1992).

Baertsch, C. D., H. H. Funke, J. L. Falconer, and R. D. Noble, "Permeation of Aromatic Hydrocarbon Vapors Through Silicalite-Zeolite Membranes," *J. Phys. Chem.*, **100**, 7676 (1996).

Bai, C., M. D. Jia, J. L. Falconer, and R. D. Noble, "Preparation and Separation Properties of Silicalite Composite Membranes," *J. Membr. Sci.*, **105**, 79 (1995).

Bein, T., and K. Brown, "Molecular Sieve Sensors for Selective Detection at the Nanogram Level," *J. Am. Chem. Soc.*, **111**, 7641 (1989).

Bein, T., K. Brown, and J. Brinker, "Molecular Sieve Films from Zeolite Silica Microcomposites," in *Zeolites: Facts, Figures, Future*, P. A. Jacobs and R. A. van Santen, eds., Elsevier Science Publishers, Amsterdam, pp. 887–896 (1989).

Caro, J., G. Finger, J. Kornatowski, J. R. Mendau, L. Werner, and B. Zibrowius, "Aligned Molecular Sieve Crystals," *Adv. Mater.*, **4**, 273 (1992).

Davis, M. E., "Zeolites and Molecular Sieves: Not Just Ordinary Catalysts," *Ind. Eng. Chem. Res.*, **30**, 1675 (1991).

Dotremont, C., B. Brabants, K. Geeroms, J. Mewis, and C. Vandecasteele, "Sorption and Diffusion of Chlorinated Hydrocarbons in Silicalite-Filled PDMS Membranes," *J. Membr. Sci.*, **104**, 109 (1995).

Feng, S., and T. Bein, "Growth of Oriented Molecular Sieve Crystals on Organophosphonate Films," *Nature*, **368**, 834 (1994).

Funke, H. H., M. G. Kovalchick, J. L. Falconer, and R. D. Noble, "Separation of Hydrocarbon Isomer Vapors with Silicalite Zeolite Membranes," *Ind. Eng. Chem. Res.*, **35**, 1575 (1996).

Gao, Z., Y. Yue, and W. Li, "Application of Zeolite-Filled Pervaporation Membrane," *Zeolites*, **16**, 70 (1996).

Geus, E. R., H. Bekkum, W. J. W. Bakker, and J. A. Moulijn, "High-Temperature Stainless Steel Supported Zeolite (MFI) Membranes: Preparation, Module Construction, and Permeation Experiments," *Microporous Mater.*, **1**, 131 (1993).

Geus, E. R., M. J. Exter, and H. Bekkum, "Synthesis and Characterization of Zeolite (MFI) Membranes on Porous Ceramic Supports," *J. Chem. Soc. Faraday Trans.*, **88**, 3101 (1992).

Hennepe, H. J. C., D. Bargeman, M. H. V. Mulder, and C. A. Smolders, "Zeolite-Filled Silicone Rubber Membranes," *J. Membr. Sci.*, **35**, 39 (1987).

Hennepe, H. J. C., W. B. F. Boswerger, D. Bargeman, M. H. V. Mulder, and C. A. Smolders, "Zeolite-Filled Silicone Rubber Membranes: Experimental Determination of Concentration Profiles," *J. Membr. Sci.*, **89**, 185 (1994).

Jansen, J. C., D. Kashchiev, and A. Erdem-Senatalar, "Preparation of Coatings of Molecular Sieve Crystals for Catalysis and Separation," in *Advanced Zeolite Science and Applications*, J. C. Jansen, M. Stocker, H. G. Karge, and J. Weitkamp, eds., Elsevier Science, Amsterdam, pp. 215–250 (1994).

Jansen, J. C., and G. M. Rosmalen, "Oriented Growth of Silica Molecular Sieve Crystals as Supported Films," *J. Cryst. Growth*, **128**, 1150 (1993).

Jansen, K. C., and E. N. Coker, "Zeolitic Membranes," *Solid State Mat. Sci.*, **1**, 65 (1996).

Jia, M. D., B. Chen, R. D. Noble, and J. L. Falconer, "Ceramic-Zeolite Composite Membranes and their Application for Separation of Vapor/Gas Mixtures," *J. Membr. Sci.*, **90**, 1 (1994).

Jia, M. D., K. V. Peinemann, and R. D. Behling, "Ceramic Zeolite Composite Membranes," *J. Membr. Sci.*, **82**, 15 (1993).

Jia, M., K. V. Peinemann, and R. D. Behling, "Molecular Sieving Effect of the Zeolite-Filled Silicone Rubber Membrane in Gas Permeation," *J. Membr. Sci.*, **57**, 289 (1991).

June, R. L., A. T. Bell, and D. N. Theodorou, "Molecular Dynamics Study of Methane and Xenon in Silicalite," *J. Phys. Chem.*, **94**, 8232 (1990).

Kapteijn, F., W. J. W. Bakker, J. van de Graaf, G. Zheng, J. Poppe, and J. A. Moulijn, "Permeation and Separation Behavior of a Silicalite-1 Membrane," *Catal. Today*, **25**, 213 (1995).

Karger, J., and D. M. Ruthven, *Diffusion in Zeolites*, Wiley, New York (1992).
Kim, S., and G. Gavalas, "Preparation of H2 Permselective Silica Membranes by Alternating Reactant Vapor Deposition," *Ind. Eng. Chem. Res.*, **34**, 168 (1995).
Kita, H., K. Horii, Y. Ohtoshi, K. Tanaka, and K. Okamoto, "Synthesis of a Zeolite NaA Membrane for Pervaporation of Water/Organic Liquid Mixtures," *J. Mater. Sci. Lett.*, **14**, 206 (1995).
Lovallo, M. C., L. Boudreau, and M. Tsapatsis, "Preparation of Supported Zeolite Films and Layers: Processing of Zeolite Suspensions and In-Situ Growth from Homogeneous Solutions," in *Microporous and Macroporous Materials*, J. S. Beck, L. E. Iton, L. E. Corbin, R. F. Lobo, M. E. Davis, S. I. Zones, and S. L. Suib, eds., MRS, Pittsburgh (in press) (1996a).
Lovallo, M. C., and M. Tsapatsis, "Nanocrystalline Zeolites: Synthesis, Characterization, and Application with Emphasis on Zeolite L Nanoclusters," in *Advanced Techniques in Catalyst Synthesis*, W. R. Moser, ed., Academic Press, in press (1996).
Lovallo, M. C., M. Tsapatsis, and T. Okubo, "Preparation of an Asymmetric Zeolite L Film," *Chem. Mater.*, **8**, 1579 (1996b).
Masuda, T., H. Hara, M. Kouno, H. Kinoshita, and K. Hashimoto, "Preparation of an A-type Zeolite Film on the Surface of an Alumina Ceramic Filter," *Microporous Mater.*, **3**, 565 (1995).
Masuda, T., A. Sato, H. Hara, M. Kouno, and K. Hashimoto, "Preparation of a Dense ZSM-5 Zeolite Film on the Outer Surface of an Alumina Ceramic Filter," *Appl. Catal. A-Gen.*, **111**, 143 (1994).
Matsukata, M., N. Nishiyama, and K. Ueyama, "Preparation of a Thin Zeolitic Membrane," in *Zeolites and Related Microporous Materials: State of the Art*, J. Weitkamp, H. G. Karge, H. Pfeifer, and W. Holderich, eds., Elsevier Science, Amsterdam, pp. 1183–1190 (1994).
Meriaudeau, P., A. Thangaraj, and C. Naccache, "Preparation and Characterization of Silicalite Molecular Sieve Membranes Over Supported Porous Sintered Glass," *Microporous Mater.*, **4**, 213 (1995).
Netke, S. A., S. B. Sawant, J. B. Joshi, and V. G. Pangarkar, "Sorption and Permeation of Acetic Acid through Zeolite Filled Membrane," *J. Membr. Sci.*, **107**, 23 (1995).
Noble, R. D., and J. L. Falconer, "Silicalite-1 Zeolite Composite Membranes," *Catal. Today*, **25**, 209 (1995).
Ozin, G. A., A. Kuperman, and A. Stein, "Advanced Zeolite Materials Science," *Angew. Chem. Int. Ed. Engl.*, **28**, 359 (1989).
Rees, L. V. C., "Exciting New Advances in Diffusion of Sorbates in Zeolites and Microporous Materials," in *Zeolites and Related Microporous Materials: State of the Art 1994*, J. Weitkamp, H. Karge, H. Pfeifer and W. Holderich, eds., Elsevier Science B.V., Amsterdam, p. 1133 (1994).
Sano, T., M. Hasegawa, Y. Kawakami, Y. Kiyozumi, H. Yanagishita, D. Kitamoto, and F. Mizukami, "Potentials of Silicalite Membranes for the Separation of Alcohol/Water Mixtures," in *Zeolites and Related Microporous Materials: State of the Art*, J. Weitkamp, H. G. Karge, H. Pfeifer and W. Holderich, eds., Elsevier Science, Amsterdam, pp. 1175–1182 (1994).
Sano, T., M. Hasegawa, Y. Kawakami, and H. Yanagishita, "Separation of Methanol/Methyl-tert-butyl ether Mixture by Pervaporation Using Silicalite Membrane," *J. Membr. Sci.*, **107**, 193 (1995).
Sano, T., Y. Kiyozumi, M. Kawamura, F. Mizukami, H. Takaya, T. Mouri, W. Inaoka, Y. Toida, M. Watanabe, and K. Toyoda, "Preparation and Characterization of ZSM-5 Zeolite Film," *Zeolites*, **11**, 842 (1991).
Sano, T., F. Mizukami, H. Takaya, T. Mouri, and M. Watanabe, "Growth Process of ZSM-5 Zeolite Film," *Bull. Chem. Soc. Jpn.*, **65**, 146 (1992).
Tsapatsis, M., and G. R. Gavalas, "A Kinetic Model of Membrane Formation by CVD of SiO_2 and Al_2O_3," *AIChE J.*, **38**, 847 (1992).
Tsapatsis, M., and G. Gavalas, "Structure and Aging Characteristics of H2-Permselective SiO_2-Vycor Membranes," *J. Membrane Sci.*, **87**, 281 (1994).
Tsapatsis, M., S. Kim, S. W. Nam, and G. Gavalas, "Synthesis of Hydrogen Permselective SiO_2, TiO_2, Al_2O_3, and B_2O_3 Membranes," *Ind. Eng. Chem. Res.*, **30**, 2152 (1991).
Tsapatsis, M., M. C. Lovallo, and M. E. Davis, "High-Resolution Electron Microscopy Study on the Growth of Zeolite L Nanoclusters," *Microporous Mater.*, **5**, 381 (1996).
Tsapatsis, M., M. C. Lovallo, T. Okubo, M. E. Davis, and M. Sadakata, "Characterization of Zeolite L Nanoclusters," *Chem. Mater.*, **7**, 1734 (1995a).
Tsapatsis, M., T. Okubo, M. Lovallo, and M. E. Davis, "Synthesis and Structure of Ultrafine Zeolite KL (LTL) Crystallites and their Use for Thin Film Zeolite Processing," in *Advances in Porous Materials*, S. Komarneni, D. M. Smith and J. S. Beck, eds., MRS, Pittsburgh (1995b).
Tsikoyiannis, J. G., and W. O. Haag, "Synthesis and Characterization of a Pure Zeolitic Membrane," *Zeolites*, **12**, 126 (1992).
Valtchev, V., S. Mintova, and L. Konstantinov, "Influence of Metal Substrate Properties on the Kinetics of Zeolite Film Formation," *Zeolites*, **15**, 679 (1995).
Vankelecom, I. F. J., E. Merckx, M. Luts, and J. B. Uytterhoeven, "Incorporation of Zeolites in Polyimide Membranes," *J. Phys. Chem.*, **99**, 13187 (1995).
Yamazaki, S., and K. Tsutsumi, "Synthesis of an A-type Zeolite Membrane on Silicon Oxide Film-silicon, Quartz Plate and Quartz Fiber Filter," *Microporous Mater.*, **4**, 205 (1995).
Yan, Y., and T. Bein, "Molecular Recognition on Acoustic Wave Devices: Sorption in Chemically Anchored Zeolite Monolayers," *J. Phys. Chem.*, **96**, 9387 (1992a).
Yan, Y., and T. Bein, "Molecular Sieve Sensors for Selective Ethanol Detection," *Chem. Mat.*, **4**, 975 (1992b).
Yan, Y., and T. Bein, "Zeolite Thin Films with Tunable Molecular Sieve Function," *J. Am. Chem. Soc.*, **117**, 9990 (1995).
Yan, Y., S. R. Chaudhuri, and A. Sarkar, "Synthesis of Oriented Zeolite Molecular Sieve Films with Controlled Morphologies," *Chem. Mat.*, **8**, 473 (1996).
Yan, Y., M. Tsapatsis, M. E. Davis, and G. R. Gavalas, "Zeolite ZSM-5 Membranes on Porous α-Al_2O_3," *J. Chem. Soc. Chem. Commun.*, **2**, 227 (1995a).
Yan, Y., M. E. Davis, and G. R. Gavalas, "Preparation of Zeolite ZSM-5 Membranes by In-Situ Crystallization on Porous α-Al_2O_3," *Ind. Eng. Chem. Res.*, **34**, 1652 (1995b).
Zones, S. I., and M. E. Davis, "Zeolite Materials: Recent Discoveries and Future Prospects," *Solid State Mat. Sci.*, **1**, 107 (1996).

Manuscript received July 17, 1996, and revision received Sept. 6, 1996.